Engineering Structures 31 (2009) 2667–2676

Contents lists available at ScienceDirect

Engineering Structures

journal homepage: www.elsevier.com/locate/engstruct

Historic bridge modelling using laser scanning, ground penetrating radar and finite element methods in the context of structural dynamics

Izabela Lubowiecka [a,*], Julia Armesto [b], Pedro Arias [b], Henrique Lorenzo [b]

[a] Department of Structural Mechanics and Bridges, Faculty of Civil and Environmental Engineering, Gdańsk University of Technology, Narutowicza 11/12, C.P. 80-952 Gdańsk, Poland

[b] Department of Natural Resources and Environmental Engineering, University of Vigo, Campus Universitario As Lagoas –Marcosende s/n, C.P. 36200 Vigo, Spain

ARTICLE INFO

Article history:
Received 17 September 2008
Received in revised form
5 March 2009
Accepted 23 June 2009
Available online 10 July 2009

Keywords:
Laser scanning
Ground penetrating radar
Finite element method
Historic structures
Dynamics
Sensitivity analysis

ABSTRACT

This paper presents a general methodology to evaluate a masonry structure, considering the fact that the geometry of the structure is complex and that material properties are unknown and cannot be directly assessed. A multidisciplinary approach is presented that integrates laser scanning, ground penetrating radar (GPR) and finite element analysis (FEM) in the documentation of a medieval masonry bridge. The complex geometry of the structure is prepared using the data collected by a laser scanner. Since the bridge internal construction is not well known, GPR techniques are used in the geometric survey to estimate its homogeneity or heterogeneity. The resulting information is used to properly define a finite element-based structural model, which is then used to model the structural behaviour of the bridge. Moreover, the sensitivity analysis of the influence of the variation of Young's modulus as a significant material parameter on the dynamic response of the bridge is performed. The study shows that this methodology has significant importance, particularly in the evaluation of the state of historic structures where, using non-invasive methods such as laser scanning and GPR is more appropriate.

1. Introduction

The topic discussed in this paper forms part of the Research Project entitled "Dimensional and structural analysis of constructions using close range photogrammetry, terrestrial laser and close range radar", Grant No BIA2006-10259, a valuable effort of the Spanish government in the documentation and analysis of medieval and Roman historic bridges in Northwest Spain. In this region, the bridges constitute a patrimonial legacy of singular value. The types of materials and forms of construction are very diverse. The historical bridges are numerous in this region of the country primarily because of the irregular orography of the landscape and population dispersion. They have played an essential role as the infrastructure of transportation and some are still in use. Nevertheless the state of conservation of many of them is deficient. Frequently, the passage of heavy, rolling traffic over these bridges has introduced excessive loads and vibrations. In addition, in many cases abandonment of the rural surroundings has caused historic bridges to be useless and forgotten. Decay, invasion of vegetation in walls, paths and other elements and extraction of pieces to be used as building material in other close constructions, are some of the problems that affect historic bridges.

The primary goal of the mentioned project is to inventory the historical bridges of Galicia, a region in Northwest Spain (see Fig. 1). The inventory includes the documentation and analysis of characteristic styles of the historic bridges dating from the roman to late medieval periods. Currently, the second phase of the project is running. It concentrates on a series of singular bridges in the inventory to perform a detailed characterization of the geometry and internal material and a structural analysis of them. The objective of this phase is to document the present state of certain emblematic bridges of the region and to develop a methodology to analyze historical bridges.

In this paper, we describe the modal analysis of the Cernadela bridge due to its importance in structural damage detection and, what follows, the heritage maintenance. The structure is located in the municipality of Mondariz, in Northwest Spain (see Fig. 1). This bridge belongs to a route that runs between historic bridges (Bridge *Remedios*, Bridge *Partidas* and Bridge *Fillaboa*) along the Tea River, surroundings that have been integrated in the Network Natura 2000 because of their natural and landscaping value.

The Cernadela Bridge has five pointed arches with the longest span of 11.5 m, upstream and downstream cutwaters with triangular section and pyramidal small hats, a double slope stone path, straight cornices and parapets of whole pieces prepared vertically. The whole structure is 74 m long and 3.7 m wide. Dating from the XVth century, it is thought that the Cernadela Bridge in its present form was raised on the remains of a Roman bridge.

* Corresponding author. Tel.: +48 600 457 142.
E-mail address: lubow@pg.gda.pl (I. Lubowiecka).

0141-0296/$ – see front matter © 2009 Elsevier Ltd. All rights reserved.
doi:10.1016/j.engstruct.2009.06.018

Fig. 1. Location of the Cernadela Bridge: Mondariz, in Northwest Spain. (From: Microsoft Virtual Earth).

In a first study of this bridge (see [1]), two finite element models were prepared based on the geometry taken from photogrammetry data. Next, structural analysis was performed to evaluate both models to emphasize the significance of the use of homogeneity or heterogeneity while modelling the bridge interior. In this paper, we develop the investigation in two advanced directions — preparing geometry and finite element modelling. We apply laser scanning equipment to obtain the structure geometry and then use the GPR data to study the internal structure of the bridge. The laser scanning facilitates to build a 3D model of the bridge as the structure is very massive and hence dimensionally reduced model cannot be applied (e.g., [2]). GPR results allow us to decide about the bridge dynamic model in the context of its heterogeneity. On that base we defined a dynamic model containing two types of building materials described by different Young's modulus. The effect of Young's modulus variation upon the structural dynamics is investigated with the aid of sensitivity analysis. Its range reflects the authors' uncertainties about the exact value.

2. 3D TLS measurement of the bridge geometry

The terrestrial techniques applicable to 3D modelling of infrastructures are basically traditional topography, close range photogrammetry and the terrestrial laser scanner (TLS). The measurement by total station is a commonly used technique, but to a great extent the quality of the resulting digital model depends on the ability of the worker to take a sufficient number of points and a suitable election of them to develop a trustworthy model of the structural elements of the bridge. The use of terrestrial photogrammetry is limited by the difficulty required to digitize points on non-regular surfaces without easily identifiable singular points; in addition, it has restrictions on the geometry of the data acquisition that are difficult to satisfy in wide rivers. Furthermore, it depends on the conditions of illumination and requires topographic support to ensure suitable precision (see e.g., [3]).

Terrestrial laser scanner (TLS) technology is starting to replace traditional geometric techniques. There are two primary types: those based on triangulation, which are short-range devices (order of meters), and those named *time of flight* laser scanners (TOF), which are long-range measuring devices (hundreds of meters up to four kilometers). The TOF scanners are applicable to the modelling and measurement of bridges and infrastructures. The measurement is based on the emission of a laser beam with a wavelength in the optical or near infrared domains that affect the object directly, so that the distance from the point of emission to the surface is obtained from the flight time of the signal. The distance measurement system is combined with a baffle plate for the ray, which aims the ray in the direction of the surface to be measured. The horizontal and vertical angles that correspond to each emitted pulse are determined by coders. Thus, a spherical coordinate system centred on the scanner is defined, from which Cartesian coordinates (X, Y, Z) are obtained for any point measured on the surface of the object.

With respect to other techniques, TLS systems offer a number of advantages: it acquires the 3D geometry of the entire surface area of an object without direct contact with the structure, which avoids alteration of the material and allows access to structural elements that may be otherwise inaccessible (vaults, central piers, etc.); it provides huge density of data (million of points), high accuracy and high rate of data acquisition. Park et al. [3] point out another essential advantage: the measurement does not require specific illumination conditions.

The combination of precision, speed and range in the same instrument has caused TLS systems to be adopted in different fields, ranging from 3D modelling and reconstruction of archaeological sites and heritage monuments [4,5], to forensic anthropologist investigations [6], urban modelling [7], or geomorphological studies [8]. In studies of infrastructure stability, the works of Park et al. [3] are relevant. They propose a procedure based on TLS for the measurement of deflections in bridges and buildings, and Kang et al. in [9] present a system of structural health monitoring.

2.1. Instrumentation

The equipment used in this work was a 3D long-range TLS (TOF) Riegl LMS-Z390i. This equipment measures distances in a range of 1.5–400 m, with a nominal precision of 6 mm, 50 m distance in normal illumination and reflectivity conditions. The vertical field of vision has an amplitude of 80 sexagesimal degrees, and 360 degrees in the horizontal plane. It has a minimum angular resolution of 0.2 degrees and a maximum of 0.002 degrees, and the rate of measurement of points oscillates between 8000 and 11,000 points per second. The software used for the recording and alignment of clouds of points is RiSCAN PRO Software, Riegl©.

This scanner is used in combination with a calibrated Nikon D200 camera. This camera incorporates a CCD sensor (Charged

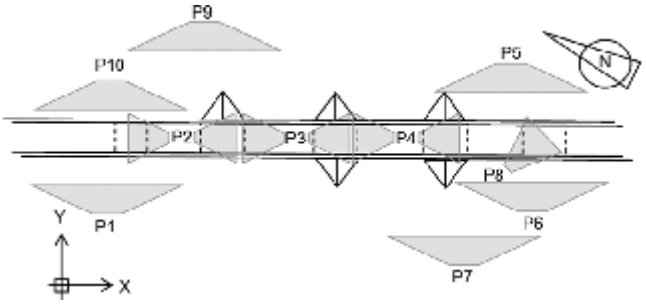

Fig. 2. Spatial distribution of scan positions.

Fig. 3. Perspective view of the whole cloud of points.

Coupled Device), DX format with 10.2 megapixels. This sensor surpasses CMOS sensors in dynamic range (relation between saturation level and threshold for the signal reception) and in terms of noise, which are both essential factors for obtaining images with sufficient quality in virtual photorealistic modelling applications. The Nikon D200 camera is equipped with a matrix color measurement system 3D II (AE) with an exhibition sensor/color RGB of 1005 pixels. The lens used for the measurement is a great angular Nikkor 20 mm f/2.8D high frequency, digital angle with a view of 70 degrees.

2.2. 3D TLS measurement

2.2.1. Acquisition project

The data acquisition was based on the necessary resolution to document the constructive elements and the damage of the structure. From a preliminary study, it was stated that cracks were present as interblock gaps and breakages; consequently, the scanning resolution was established in 2 mm for the documentation of damages and 2 cm for the generation of a general model of the bridge. This leads to the acquisition of two scans for each position: one scan of low resolution, that should correspond with 0.05 degrees angular interval to 20 m distance between bridge and scanner; a detailed scan should satisfy 0.0057 degrees to 20 m.

Another factor that affected data acquisition was the occlusion factor. In a bridge, the conditions of accessibility to establish scan positions are restricted to the river sides, but it is necessary to consider occlusions due to the cutwaters, as well as the visibility of vaults.

2.2.2. Data acquisition

Before initiating the scans, two operations were performed:

– Connection of the digital camera to the scanner by means of an external support. The parameters of rotation and translation were estimated to transfer the coordinate system centred in the camera to the one centred in the scanner. For this end 11 reflecting targets, 5 cm diameter, were placed around the instrument at a distance less than 10 m. They were precisely scanned and photographed with minimum aperture, maximum speed and flash. By means of enhancement systems, the targets were detected in the scan and in the images, and the parameters of translation and rotation were estimated. An error RMS in the adjustment of 0.4 pixels was obtained.

– Reference targets were distributed on the surface of the object to be measured so that there were at least four common targets in each pair of scans. The coordinates of each of these targets were measured by means of total station in order to accurately levelling the global cloud of points and to improve the result of alignment of single scans.

Ten scan positions were established (Fig. 2). At each position, the following operations were performed:

– A low resolution scan for the construction of the geometric model of the bridge. The bridge walls were scanned from positions 1, 5, 7, and 9. Scans 6, 8, and 10 allowed the occluded zones to be completed. Scans 2, 3 and 4 provided the path information. As each scan has an empty cone under the scanner due to the vertical amplitude of the scanner ($+/-40°$), when the scanner is placed on the surface to be modelled, as the bridge path, it is precise to scan this position from the following one.

– Detailed scan for the documentation of structural damages. Another 10 detailed scans were done with 2 to 5 mm of spatial resolution.

– Detailed scans of reference targets (used for alignment of clouds of points). Eleven targets were used with 10 cm diameters, and they were scanned with 1000 to 3000 points for the estimation of their centres with maximum precision.

– Image acquisition designed to determine the texture of the final 3D surface model. Between 12 and 15 images of the bridge and surroundings were taken from each position. Twenty-four were used for texturing of the cloud of points and the final 3D model.

2.2.3. Data processing

The processing of clouds of points was carried out in the following phases:

– Alignment of point clouds in a common coordinate system. This was carried out by means of common targets between successive scans combined with a surface matching system based on the iterative closest point (ICP) algorithm (see [10]). The standard deviation of errors in the global alignment was 6.6 mm. Fig. 3 shows the low resolution clouds of points aligned in a common coordinate system. The whole cloud included more than 33 million points.

– Cleaning and segmentation. Isolated points were eliminated, the mesh was regularized and the global cloud of points was divided into bridge and surrounding categories.

– Triangulation. In order to develop a 3D model of the surfaces of the bridge, a 2D Delaunay flat triangulation was applied to each wall of the bridge with respect to the visualization plane, limiting the length of the edges to 1 m and the angle between rays to 5 degrees.

– Texturing of the surface model. In order to assign a texture to a triangle, one image is selected that satisfies three criteria: minimum distance between camera position and the centre of each triangle, visibility of the triangle in the image and minimum angle of view. Thus, a photorealistic 3D surface model is obtained, from which ortho-images of the bridge can be generated. These ortho-images can be exported to programs such as CAD, or used to obtain the real measures.

2.3. Results

The scan of the bridge lasted a complete day. Low resolution scans required 5 to 10 min, while high resolution scans needed 30 to 45 min. The registry of the position of the support of the camera with respect to the scanner requires about 20 min.

From the 3D surface model, ortho-images were generated that realised the corresponding metric analysis of the bridge (see Fig. 4 and Table 1) and a solid model was built for the further structural analysis.

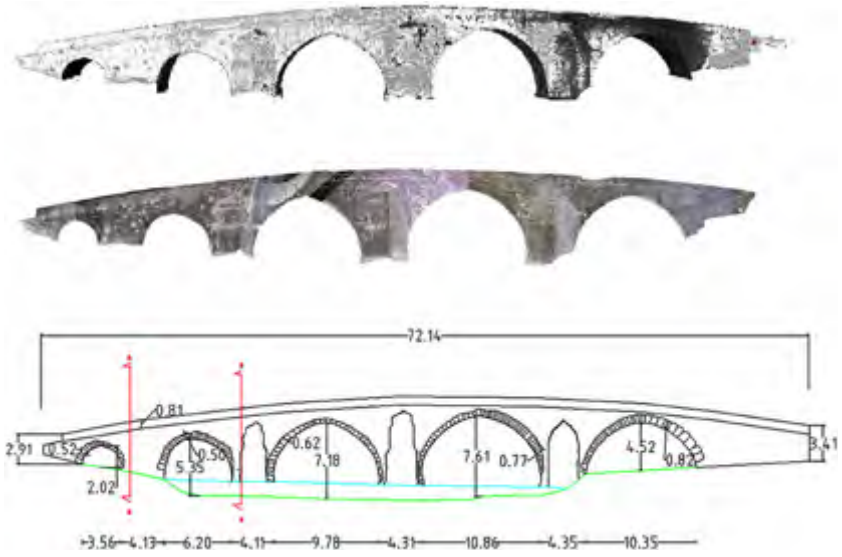

Fig. 4. Front view of the 3D surface model, the photorealistic 3D model and the wire frame model.

Table 1
Dimensional analysis of the Cernadela Bridge.

Arch	Span		Height		Thickness of arch pieces	
	DS	US	DS	US	DS	US
1	10.20	10.36	4.55	4.42	0.84	0.73
2	11.07	11.18	7.50	7.60	0.74	0.61
3	9.76	9.74	6.98	7.10	0.67	0.52
4	6.35	6.33	5.31	5.07	0.47	0.59
5	3.63	3.59	1.93	1.89	0.47	0.37

Piers	Width		Distance between axes	
	US	DS	US	DS
1	4.30	4.16	15.40	15.35
2	4.47	4.11	14.00	13.89
3	3.87	4.03	10.18	10.28
4	4.14	4.34		

Cutwater	US					DS				
	Width	Left	Right	Ang1	Ang2	Width	Left	Right	Ang1	Ang2
1	5.01	2.52	2.49	37	37	4.16	2.26	1.90	39	37
2	4.00	2.55	1.45	39	26	4.00	1.99	2.01	39	40
3	4.00	2.45	1.55	38	26					

Other elements	Length	Height	Width
Stirrups DS left/right	3.36/2.93		
Stirrups US left/right	2.99/4.31		
Parapet DS		0.84	
Parapet US		0.70	
Road path			3.85

3. Ground penetrating radar tests of the bridge internal structure

The next step in the bridge evaluation procedure leading to information about its internal structure is the radar test. Ground penetrating radar (GPR) is a remote sensing and geophysical method based on the emission of very short electromagnetic pulses (1–20 ns) in the frequency band of 10 MHz to 5 GHz (Fig. 5). GPR equipment usually consists of a laptop, a control unit and an ultra-wideband antenna. By moving the antenna over the ground, an image of the shallow subsurface under the displacement line is obtained. These images, called radargrams or B-scans, are X–Z graphic representations of the detected reflections, where the X-axis represents antenna displacement and the Z-axis represents the two-way travel time of the emitted pulses.

Fig. 5. Main components of a GPR system: control unit, laptop and antenna.

Depending on the depth being investigated and the required resolution, different antenna frequencies are selected. In general, as the frequency of the antenna increases so does the resolution, but the capacity of penetration of the signal decreases [11]. Resolution can be understood, as proposed by Annan [12], as the radar system's capacity to discriminate individual elements in the subsoil. Given an antenna with a particular central frequency, an estimation of the expected resolution and penetration depth in typical soil materials is presented in Table 2.

3.1. Methodology

The GPR data was collected using a RAMAC GPR system equipped with 250 and 500 MHz shielded antennas. Three parallel longitudinal profiles were recorded with each antenna, giving six 108 m long radargrams. The distance between profiles was set to 1 m. Taking into account the characteristics of each antenna in terms of penetration depth and resolution (Table 2), data was acquired with trace intervals of 5 and 2 cm, and time windows of 220 and 100 ns, for the 250 and 500 MHz antennas, respectively. During the survey, an odometer wheel was used to accurately position the radar data (Fig. 6).

Obtained radargrams were processed following a general processing sequence consisting of dewow (DC removal), max phase

Fig. 6. The GPR survey consisted of three parallel profiles 1 m apart using 500 and 250 MHz shielded antennas.

Table 2
Resolution and maximum penetration depth versus antenna frequency [30].

Centre frequency (MHz)	Resolution (m)	Max. penetration (m)
10	2	60
25	1	50
50	0.5	40
100	0.25	25
200	0.125	12
500	0.05	6
800	0.03	2.5
1000	0.025	1.5

correction, band pass filtering, geometrical divergence compensation and topographic correction. For topographic correction and time–depth conversion of the radargrams, an average velocity of 11 cm/ns, which was obtained from the structural dimensions of the bridge provided by the dimensional analysis of the TLS 3D model of the bridge, was used.

To facilitate the identification of different areas in the bridge in terms of heterogeneity, an additional processing flow based on the calculation of the first derivative and envelope (Hilbert-transformation) of the data in the temporal direction was used. The interpretation of each radargram processed in this way was combined in a pseudo-3D model to obtain a rough composition of the bridge's internal structure.

3.2. Results

Fig. 7 shows the profiles gathered with the 250 MHz antenna after a basic processing sequence. The main structural elements of this construction are clearly defined in the radargrams, giving a first insight into the internal structure of the bridge.

Fig. 8 shows an example of the interpretation process. Once each profile is filtered following a more specific processing flow, areas with strong reflectors in the data are manually interpreted as coarse fill materials inside the bridge.

As shown, the coarse fill material, arch stones and air-water interface can be clearly discriminated. This should be enough to consider that the material properties of the fill of the bridge structure and the main external layer (spandrel) are different. However, it should be highlighted that material properties of historic structures strongly depends not only on the distribution of material interfaces but also on the content of moisture and salinity of water.

All these GPR data are used to build 3D finite element model considering non-homogeneous internal structure of the bridge, performed in the next section.

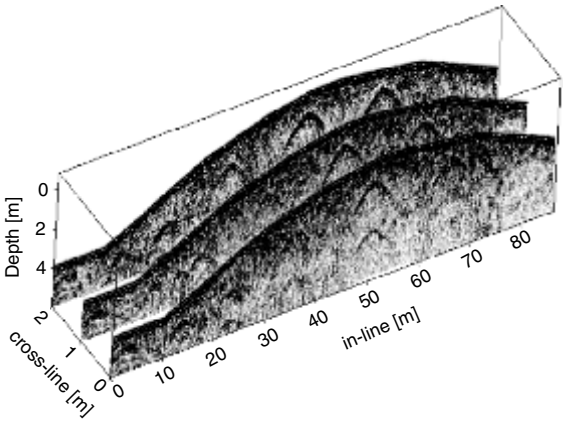

Fig. 7. B-Scans obtained with the 250 MHz antenna.

4. Finite element modelling and modal analysis

Increase in transport capacity demand, deterioration of materials and identification of a variety of defects have resulted in the recent past in the need for assessment and maintenance procedures for existing masonry bridges. More than ever, bridge structures are subjected to intense urban influence like overloaded traffic together with bad conditions. For this reason, it is important to measure and calculate structural vibration, as well as to specify a resonance range to avoid a structural collapse, and proceed to a rehabilitation process or introduce some traffic restrictions if necessary. In order to perform the mechanical behaviour of these structures, the finite element analysis together with on site testing is an useful tool. Often, FEM analysis results are difficult to interpret from a practical engineering point of view when represented by a continuum model [13]. This gives a qualitative idea of where stresses are concentrated (e.g., [14]). An easier situation appears when modal analysis is considered. In this situation, the values of the eigenfrequencies and the shapes of the modes are usually given directly from the analysis [15].

In this study the authors consider the modal analysis of a medieval bridge owing to its considerable meaning in damage recognition (e.g., [16]). Also modal analysis along with on site measurement can be applied to calibration of the numerical model what makes the computer simulation more reliable.

4.1. Methodology

There are different modelling strategies that may be used for masonry structures. Principal components of a typical masonry bridge, such as vaults, piers, fill and spandrels, can be considered as simple 2D models based on beam, triangular and interface elements. Such a complex 3D system, whose interacting components are made up of different kinds of masonry and soil materials can be modelled by finite elements which include appropriate consistent constitutive laws (e.g., [17]). Ideally, the analyst would represent each physical unit with the element of mechanical properties of the unit material — stones and mortar models with cohesion between blocks [18]. Nevertheless, to reduce the costs of analysis, we consider a continuous 3D finite element model (e.g., [14,19]) based on the geometry taken from TLS described in Section 2. The laser scanned geometry data after all post-processing procedure are used for building the structural geometry of the bridge model which is applied in the FEM software.

Since only non-destructive test methods are available, the GPR radar test gives important general information about the internal structure of the bridge. We cannot define details but we can decide about its internal homo or heterogeneous structure. In this context,

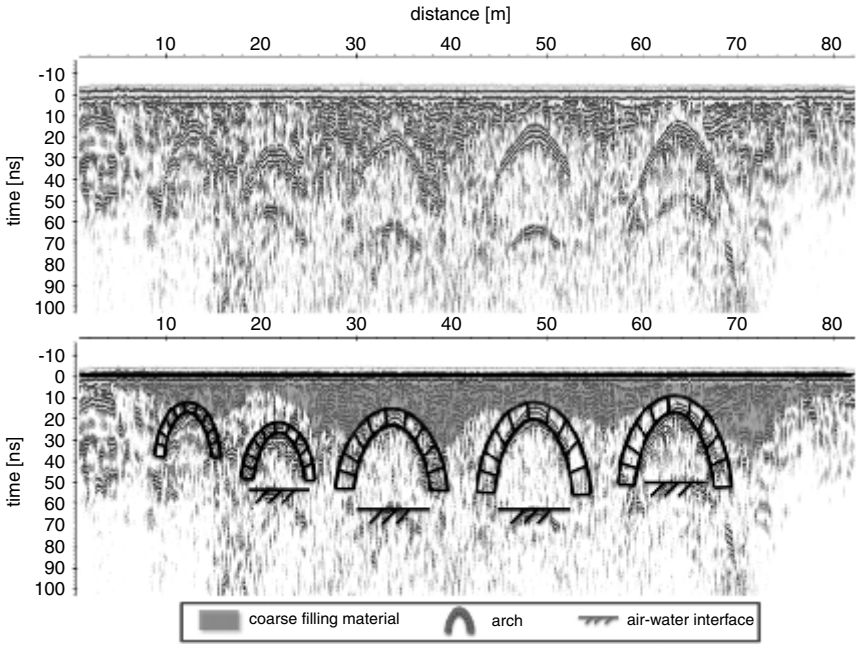

Fig. 8. Processed B-Scan (up) and subsequent interpretation (down) of a profile recorded with the 250 MHz antenna (Note that in this example data is not topographically corrected).

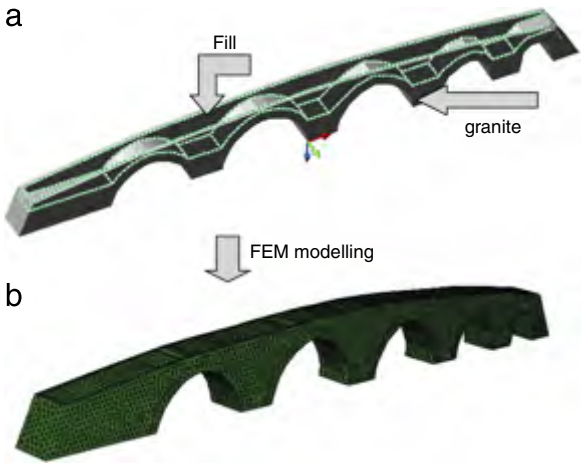

Fig. 9. (a) 3D model (b) FEM model of the Cernadela Bridge.

heterogeneity means that the material properties of the fill of the bridge structure and the main external layer (spandrel) are different. The model (Fig. 9) is a combination of two parts made of different materials to simulate differences between the external layer (spandrel) of the structure with five load carrying arches and the inside (fill) [1].

As Young's modulus of the building materials for these kinds of historic bridges can significantly differ for various structures, we consider it to have a range of 15–23 GPa for this analysis. We cannot properly specify Young's modulus E of every part of the bridge, so we assume external layers of the bridge, as well as the supports and arches, are modelled in granite ($E = 23$ GPa) and the modulus of the fill varies from 15 to 23 GPa (e.g., [13]). The masonry and fill density is considered to be $\gamma = 22.000\ \mathrm{N/m^3}$, and the Poisson ratio of both components is $\nu = 0.2$, as described by Cavicchi and Gambarotta [17]. The maximal value of Young's modulus (23 GPa) of the fill makes the model homogeneous because the whole structure has the same value in this case. The significance of Young's modulus in the modal analysis of this kind of ancient structure will be investigated by means of sensitivity analysis (e.g., [20]). An important problem in modelling masonry structures is the choice of a constitutive model what has a wide reflection in literature [21–23]. A set of linear elastic material parameters and specific non-linear material laws define the material properties for the masonry and the fill component, e.g. non-linear isotropic models including brittle behaviour in tension and plastic behaviour in compression (see e.g., [21]). In the paper by Fanning and Boothby [22] the performance of structural masonry is characterized by high compressive strength with little or no tensile strength it is replicated by the use of solid element that can have its stiffness modified by the development of cracks and crushing. The fill is modelled by Drucker–Prager material, and the interface between the masonry and the fill is characterized as a frictional contact surface.

At this stage of analysis, the material is treated as isotropic linear and elastic. The analysis is carried out in the ABAQUS/Standard calculation system with the use of 3D structural continuum (solid) stress/displacement elements. The element type used here is a 4- and 10-node linear tetrahedron as well as a 8- and 20-node brick having three degrees of freedom in each node with three translations in the x, y and z directions. First-order tetrahedrons have a simple, constant-strain formulation, and very fine meshes are required for an accurate solution (e.g., [24]). The convergence analysis was performed (cf. [1]), and the highest element number considered in the calculations was 46,075 with a total number of degrees of freedom (dof) = 390,111.

4.2. Finite element results

In the modal analysis of the structure, the first 15 eigenmodes were considered. The detailed results of the simulations of the structural behaviour for two different FEM models of Cernadela Bridge are shown in [1]. Note the horizontal character of the first mode shape which is opposite to the vertical vibration shape typical for modern constructions, which was also presented in [2] (see Fig. 10).

It is important to emphasize how the eigenmodes and eigenfrequencies strongly depend on the material properties that is also well addressed in [2,25,26]. The influence of the changes of Young's modulus internally is shown in Fig. 11.

Fig. 10. 1st eigenmode of the Cernadela Bridge model.

As Young's modulus of the fill increases, the natural frequency values also increase. The first natural frequency value starts with the value $\lambda_1^{E=15} = 5.85$ Hz for the value of Young's modulus of the internal part of the bridge $E = 15$ GPa. This value, with a change of Young's modulus to $E = 23$ GPa, increases to $\lambda_1^{E=23} = 5.99$ Hz. In particular, the growth of the eigenfrequencies is noticeable for further modes. The highest spread of the frequency values is evident for the 8th one (from $\lambda_1^{E=15} = 16$ Hz to $\lambda_1^{E=23} = 17.1$ Hz) and 13th one (from $\lambda_1^{E=15} = 20.81$ Hz to $\lambda_1^{E=23} = 22.32$ Hz), which is shown in Fig. 12.

However, the shapes of the eigenmodes do not change with the growth of E. This phenomenon was observed in the case of changes of Young's modulus together with fill density (e.g., [1]). On the other hand, even for the early natural frequencies we can observe the essential difference in the range of deformation (e.g., Fig. 13).

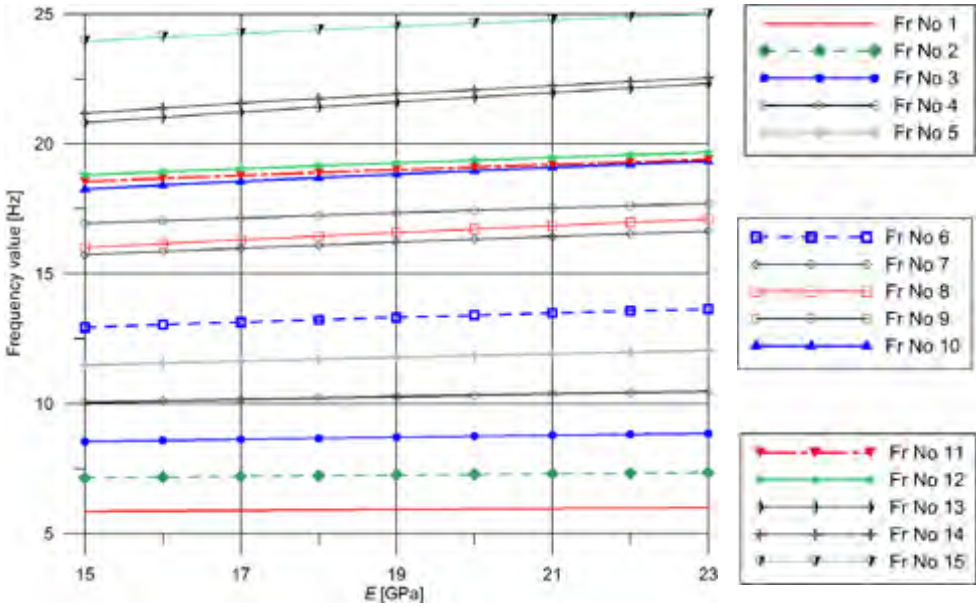

Fig. 11. Frequencies vs. Young's modulus.

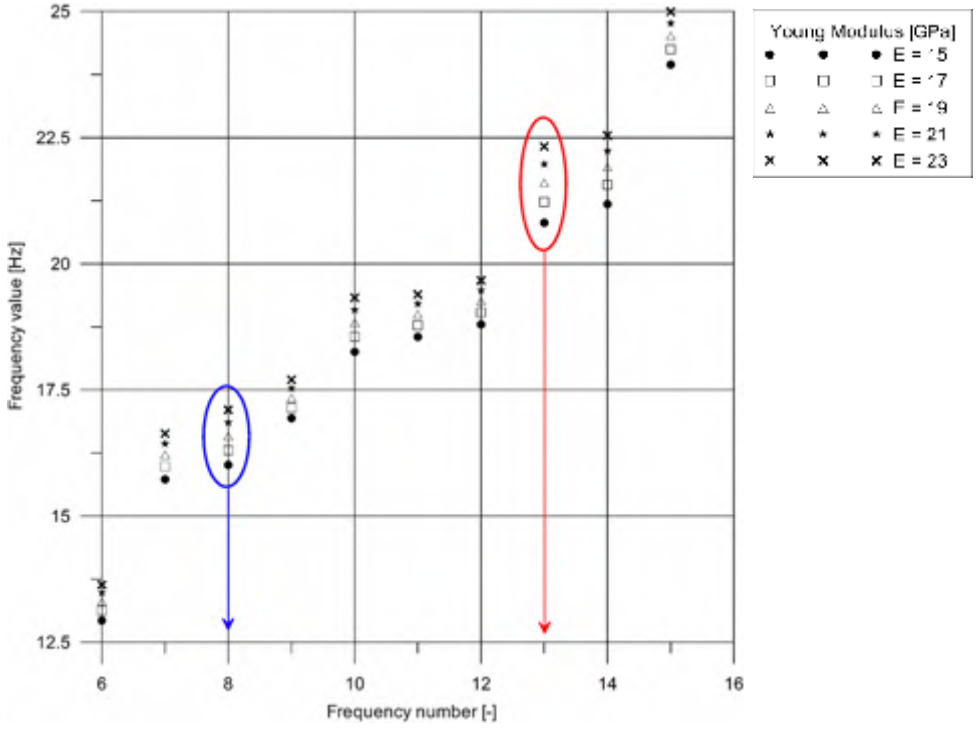

Fig. 12. Changes in natural frequency values vs. frequency number for different values of Young's modulus.

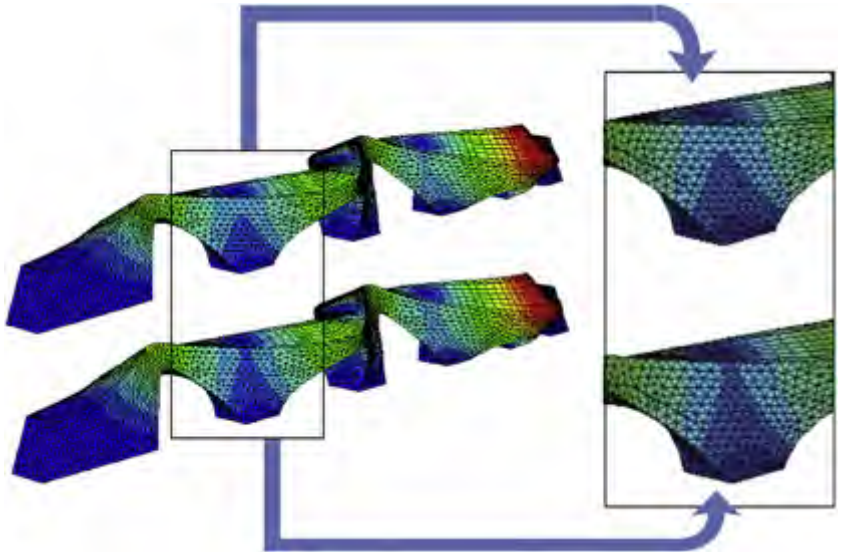

Fig. 13. Discrepancies in the deformation of the bridge structure with Young's modulus $E = 23$ GPa (up) and $E = 15$ GPa (down) — the 4th eigenmode.

4.3. Sensitivity analysis

Sensitivity analysis is a powerful tool in engineering design and many of its applications are described by Szymczak [20]. In this research, we plan to assess the importance of Young's modulus as a parameter that affects the structural dynamics of the Cernadela Bridge [27]. There are variety of other material parameters characterizing the behaviour of masonry structures e.g., fracture energy, shear and tensile strength, friction factor, elastic limit in compression, shear modulus, which have prevailingly non-linear nature [23]. Nevertheless, owing to the local character of performed sensitivity analysis we do not consider the material behaviour in overall range of strain but, only near the actual state of stress. Here, the linearization reveals proper results and the influence of parameters causing non-linear effects like cracks and fracture etc., have not so significant meaning.

The dynamic analysis of the bridge for Young's modulus of the fill, varying from 15 to 23 GPa, is carried out by means of commercial FEM software. The analysis of sensitivity of eigenfrequencies due to the variation of Young's modulus (as a parameter) of the fill material is performed by means of the method presented by Chen and Ho [28]. In this method, the derivative is calculated directly from the definition using the results of FEM software, even if the software used here does not provide a design sensitivity analysis capability (see also [29]).

The derivative of the natural frequencies relative to the change of Young's modulus is assumed to be calculated according to central difference equation (1).

$$\delta\lambda_j = \frac{\lambda(E+\delta E) - \lambda(E-\delta E)}{2} = W_{jE}\delta E, \tag{1}$$

where E is Young's modulus, δE is a perturbation of Young's modulus, W_{jE} represents a sensitivity coefficient and λ_j is a natural frequency value. The relative value of the variation is described as follows:

$$\frac{\delta\lambda_j}{\lambda_j} = \frac{\lambda(E+\delta E) - \lambda(E-\delta E)}{2\lambda_j} = W_{jE}\frac{\delta E}{\lambda_j}, \tag{2}$$

where λ_j is a initial natural frequency value corresponding to the initial value of Young's modulus E. After some further transformations, the formula becomes

$$\frac{\delta\lambda_j}{\lambda_j} = \frac{\lambda(E+\delta E) - \lambda(E-\delta E)}{2\lambda_j} = W_{jE}\frac{E}{\lambda_j}\frac{\delta E}{E} \tag{3}$$

and represents the relative variation of frequency in relation to the relative change of Young's modulus.

Let us introduce the following symbols:

$$\frac{\delta\lambda_j}{\lambda_j} = \delta\bar{\lambda}_j, \qquad \frac{\delta E}{E} = \delta\bar{E}, \qquad \bar{W}_{jE} = W_{jE}\frac{E}{\lambda_j} \tag{4}$$

that yield

$$\delta\bar{\lambda} = \bar{W}_{jE}\delta\bar{E}. \tag{5}$$

This gives us the relative coefficient of sensitivity of natural frequencies $\bar{W}_{jE}$ for different values of Young's modulus. The influence of the E parameter variation to the dynamic response of the structure is presented in Fig. 14 (for the first 5 frequencies) and Fig. 15 (for the 6th–15th frequencies) as a coefficient of relative variation of frequency vs. Young's modulus.

The sensitivity analysis reveals that the highest influence appears in the higher natural frequencies (like the 13th, 8th and 14th) and the lowest influence is observed in the 1st and 3rd frequencies. This is important due to the fact that the most significant natural frequencies of the structures are the first ones. Even if the frequencies increase with the growth of E, their sensitivity decreases, which is indicated by the decreasing character of the sensitivity function plot.

5. Conclusions

In this paper, we show the methodology of the test of historic structures in three steps: geometric data collection (laser scanning); internal structure (GPR) description; and finally, structural analysis (FEM).

The data collected from the laser scanner is used to measure and model heritage bridges. This technology is very useful, especially when the structural analysis requires a complete and accurate 3D model. Against the conventional terrestrial techniques (topography and photogrammetry), TLS systems have the advantage of not depending on a worker to choose the points to measure on the surrounding surface of the skittle. The intervention of the user is restricted to the configuration of the angular resolution of a scan. Another important advantage of this system is that the TLS allows a volume of points thousands of times superior the traditional procedures to be captured, in addition to providing Cartesian coordinates in real time. The registry of point clouds and meshes allows graphic documents in conventional formats to

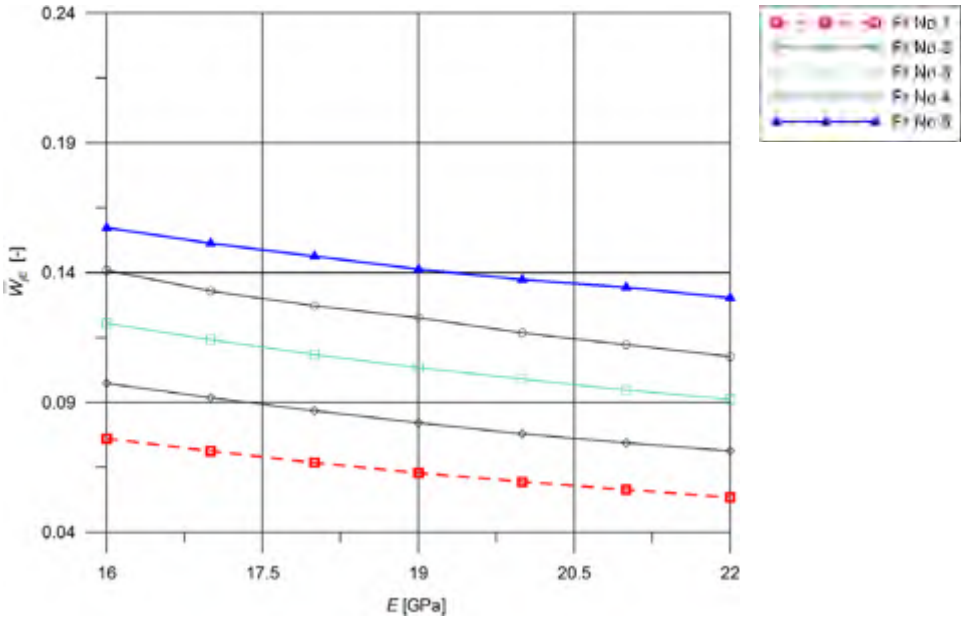

Fig. 14. Coefficient of relative variation of frequency (1–5) vs. Young's modulus.

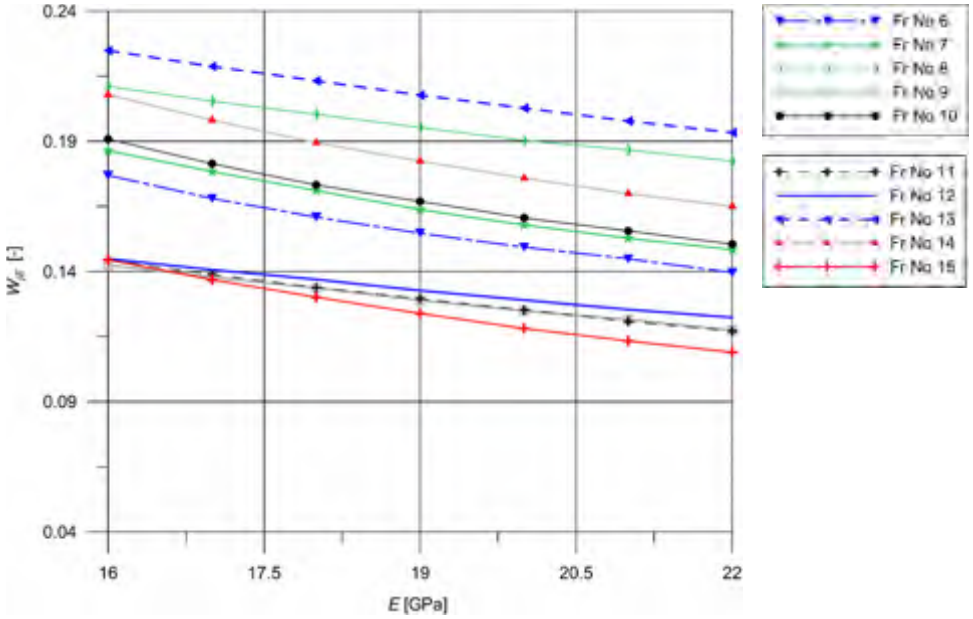

Fig. 15. Coefficient of relative variation of frequency (6–15) vs. Young's modulus.

be obtained, as well as very accurate performance measurements. This is a technique of great interest in the field of the bridge documentation, modelling, and measurement.

The Ground Penetrating Radar technique aids in estimating the internal structure of the historic bridge and determine the preparing of finite element model. It is of great importance in the case when the use of destructive method of testing is not available. The interpretation of the GPR data is used as a starting point to build a hypothesis for the numerical model and the finite element structural analysis.

The modal analysis reveals that the obtained range of the natural frequencies as well as the character of 1st mode of Cernadela Bridge is typical for massive masonry structures. Moreover, it has been observed that the value of Young's modulus is a significant parameter in the FEM modelling of the considered bridge. Owing to the different frequency values, as well as mode shapes, it is clear that the variation of Young's modulus causes the models to vary, and the consideration of GPR data in the finite element modelling affects the results. However, the proper decision on how to prepare the representative model of the tested structure relies on measurements of the natural vibrations of the bridge. In structural dynamics, the most important eigenmodes are the first ones. Since Young's modulus values used affect the highest natural frequencies, practicing engineers should consider the acceptable range of these discrepancies with respect to the modelling and calculation costs.

The authors' future study will be to identify the real values of the natural frequencies of the bridge structure to compare with computational results and to adapt the FEM model on the basis of these data.

Acknowledgements

The financial support of the Ministry of Science and Education (Spain), for Scientific Research under Grant No BIA2006-10259 (Title: "Dimensional and structural analysis of constructions using close range photogrammetry, terrestrial laser and close range radar") is gratefully acknowledged.

Computations were done at the TASK Computer Science Centre, Gdańsk, Poland.

References

[1] Lubowiecka I, Armesto J, Rial FI, Arias P. Masonry bridge FEM modelling based on Digital Photogrammetry and GPR tests. In: Topping BHV, Papadrakakis M, editors. Proceedings of the ninth international conference on computational structures technology. Stirlingshire (Scotland): Civil-Comp Press; 2008.
[2] Zeman J, Novák J, Šejnoha M, Šejnoha J. Pragmatic multi-scale and multi-physics analysis of Charles Bridge in Prague. Eng Struct 2008;30:3365–76.
[3] Park HS, Lee HM, Adeli H, Lee I. A new approach for health monitoring of structures: Terrestrial laser scanning. Comput Aided Civil Infrastruct Eng 2007;22(1):19–30.
[4] Yastikli N. Documentation of cultural heritage using digital photogrammetry and laser scanning. J Cultural Heritage 2007;8(4):423–7.
[5] Guidi G, Frischer B, Russo M, Spinetti A, Carosso L, Micoli L. Three-dimensional acquisition of large and detailed cultural heritage objects. Mach Vis Appl 2006; 17(6):349–60.
[6] Bolliger SA, Thali MJ, Ross S, Buck U, Naether S, Vock P. Virtual autopsy imaging: Bridging radiologic and forensic sciences, A review of the Virtopsy and similar projects. European Radiol 2008;18:273–82.
[7] Barber D, Mills J, Smith-Voysey S. Geometric validation of a ground-based mobile laser scanning system. ISPRS J Photogram Remote Sensing 2008;63(1): 128–41.
[8] Abellán A, Vilaplana JM, Martínez J. Application of a long-range Terrestrial Laser Scanner to a detailed rockfall study at Vall de Núria (Eastern Pyrenees, Spain). Eng Geol 2008;88:136–48.
[9] Kang DS, Lee HM, Park HS, Lee I. Computing method for estimating strain and stress of steel beams using terrestrial laser scanning and FEM. Key Engineering Materials 2007;347:517–22.
[10] Besl P, McKay NA. Method for registration of 3-d shapes. IEEE Trans Pattern Anal Machine Intell 1992;14(2):239–56.
[11] Daniels D. Ground penetrating radar. 2nd ed. London: IEE; 2004.
[12] Annan AP. Ground penetrating radar: Principles, procedures & applications. Mississauga: Sensors & Software Inc.; 2003.
[13] Binda L, Lenzi G, Saisi A. NDE of masonry structures: Use of radar tests for the characterization of stone masonries. NDT&E Int 1998;31:411–9.
[14] Arias P, Armesto J, Di-Capua D, González-Drigo R, Lorenzo H, Pérez-Gracia V. Digital photogrammetry, GPR and computational analysis of structural damages in a mediaeval bridge. Eng Failure Anal 2007;4(8):1444–57.
[15] Armesto J, Lubowiecka I, Ordóñez C, Rial F. FEM modeling of structures based on close range digital photogrammetry. Automation in Construction 2009;18: 559–69.
[16] Petryna YS, Kraetzig WB. Compliance-based structural damage measure and its sensitivity to uncertainties. Comput & Structures 2005;83:1113–33.
[17] Cavicchi A, Gambarotta L. Collapse analysis of masonry bridges taking into account arch–fill interaction. Eng Struct 2005;27:605–15.
[18] Rafiee A, Vinches M, Bohatier C. Application of the NSCD method to analyse the dynamic behaviour of stone arched structures. Internat J Solids Structures 2008;45:6269–83.
[19] Bull JW, editor. Computational modelling of masonry. Brickwork and Blockwork Structures Saxe-Coburg Publications; 2001.
[20] Szymczak C. Elements of design theory. Warsaw: PWN; 1998 [in Polish].
[21] Romera LE, Hernandez S, Reinosa JM. Numerical characterization of the structural behaviour of the Basilica of Pilar in Zaragoza (Spain). Part 1: Global and local models. Adv Eng Softw 2008;39:301–14.
[22] Fanning PJ, Boothby TE. Three-dimensional modeling and full-scale testing of stone arch bridges. Comput & Structures 2001;79:2645–62.
[23] Berto L, Saetta A, Scotta R, Vitaliani R. Shear behaviour of masonry panel: Parametric FE analyses. Internat J Solids Structures 2004;41:4383–405.
[24] Juhasova E, Sofronie R, Bairrao R. Stone masonry in historical buildings—Ways to increase their resistance and durability. Eng Struct 2008;30:2194–205.
[25] Bathe KJ. Finite element procedures. New Jersay: Prentice Hall; 1996.
[26] Colla C, Brencich A. The influence of construction technology on the mechanics of masonry railway bridges. In: Proceedings of railway engineering conference. 2002.
[27] Gentile C, Saisi A. Ambient vibration testing of historic masonry towers for structural identification and damage assessment. Constr Build Mater 2007;21: 1311–21.
[28] Chen JL, Ho JS. A comparative study of design sensitivity analysis by using commercial finite element programs. Finite Elem Anal Des 1994;15:189–200.
[29] Iwicki P. Stability of truss with linear elastic side-supports. Thin-Walled Struct 2007;45:849–54.
[30] RAMAC GPR user manual, Mala Geoscience. www.malags.se.